where ρ is atmospheric density, V the speed relative to the atmosphere, A the effective cross-sectional area of the rocket, and C_D the coefficient of drag (which depends on Mach number primarily). We shall assume that C_D is invariant to scaling so that the only drag parameter to be scaled is A.

If we let μ be the ratio of the final to initial weight of a single stage rocket, t the burning time, and s the time from initiation of burning, then mass m is given by

$$m = h(t - s + \mu s)(1 - \mu)^{-1}$$

where h is the mass burning rate (assumed independent of s). Reference to the equations of motion shows that they will be invariant to payload changes if the parameters t, μ, a/h, and A/h are kept invariant (in addition to those specified previously). Under these conditions, it is evident that for any given value of p the function $Fh^{-1}g^{-1} = I$ = specific impulse will be invariant as stated previously (g is the mass-to-weight conversion factor). From the preceding definitions, we have $gh = t^{-1}W(1 - \mu)$, where W is the initial weight. Then the invariants a/h and A/h can be replaced by the invariants a/W and A/W.

For an n stage rocket, let W_L denote payload weight, w_i the initial weight of the ith stage (without any upper stages), W_i the initial weight of the ith rocket (weight of ith stage plus all upper stages and payload), I_i the specific impulse of the ith stage, σ_i the final to initial weight ratio of the ith stage, and μ_i the final to initial weight ratio of the ith rocket.

By definition,

$$\mu_i = \frac{W_{i+1} + \sigma_i w_i}{W_i} = 1 - (1 - \sigma_i)\frac{w_i}{W_i}$$

$$W_i = w_i + w_{i+1} + \ldots w_n + W_L$$

If Δ denotes a change in a quantity, we obtain from the preceding the following scaling laws:

$$(1 - \mu_i)\Delta W_i = \Delta w_i - \Delta(\sigma_i w_i)$$

$$\Delta a_i = (a_i/W_i)\Delta W_i \qquad \Delta A_i = (A_i/W_i)\Delta W_i$$

$$\Delta F_i = (F_i/a_i)\Delta a_i$$

In general, the stage weight at burnout can be expressed as

$$\sigma_i w_i = \omega_{xi} + \alpha_i w_i + \beta_i F_i$$

which states that the burnout weight contains a portion ω_{xi} independent of stage weight and thrust, a portion $\alpha_i w_i$ dependent upon the stage weight (fuel tanks and structure), and a portion $\beta_i F_i$ dependent upon the thrust level (the rocket motor and pumps). Consequently, if we assume ω_{xi}, α_i, and β_i are not to be scaled, $\Delta(\sigma_i w_i) = \alpha_i \Delta w_i + \beta_i \Delta F_i$. For a wide variety of rockets, it can be assumed that $\alpha_i \simeq 0.1$ and $\beta_i \simeq 0.01$.

Scaling Laws for a Two-Stage Rocket

Using the preceding scaling laws and the invariance of t_i, μ_i, ω_{xi}, α_i, and β_i, we obtain for a two-stage rocket (in which one stage is in the atmosphere)

$$\Delta I_1 = \Delta I_2 = 0$$

$$\Delta F_1 = (F_1/W_1)\Delta W_1 \qquad \Delta A_1 = (A_1/W_1)\Delta W_1$$

$$\Delta a_1 = (a_1/W_1)\Delta W_1$$

$$\Delta F_2 = (F_2/W_2)\Delta W_2 \qquad \Delta a_2 = (a_2/W_2)\Delta W_2$$

$$\Delta W_1 = \Delta w_1 + \Delta W_2 \qquad \Delta W_2 = \Delta w_2 + \Delta W_L$$

$$\Delta w_1 = \left(1 - \mu_1 + \frac{\beta_1 F_1}{W_1}\right)\left(\mu_1 - \alpha_1 - \frac{\beta_1 F_1}{W_1}\right)^{-1} \times (\Delta w_2 + \Delta W_L)$$

$$\Delta w_2 = \left(1 - \mu_2 + \frac{\beta_2 F_2}{W_2}\right)\left(\mu_2 - \alpha_2 - \frac{\beta_2 F_2}{W_2}\right)^{-1} \Delta W_L$$

Using $-\dot{w}$ to denote weight rate of propellant consumption ($\dot{w}$ is a negative quantity), we also have

$$\Delta(-\dot{w}_1) = (1 - \mu_1)t_1^{-1}\Delta W_1$$

$$\Delta(-\dot{w}_2) = (1 - \mu_2)t_2^{-1}\Delta W_2$$

If the $\dot{w}_i$ are the design parameters rather than the σ_i, it is convenient to calculate μ_i from $\mu_i = 1 + \dot{w}_i t_i / W_i$.

Example

The preceding scaling laws were applied to a typical two-stage ICBM using a realistic physical model of the rocket and its environment, including a rotating oblate earth with a standard atmosphere and variation of the coefficients of lift and drag with Mach number. A nominal booster power flight trajectory for a 4500-lb payload was simulated on the digital computer. Then the payload was reduced by 700 lb and the scaling laws used to determine the following changes in the booster parameters:

$\Delta F_1 = -32{,}750$ lb	$\Delta F_2 = -6706$ lb
$\Delta A_1 = -8.6$ ft^2	$\Delta a_1 = -334$ in.^{2}
$\Delta \dot{w}_1 = 131$ lb/sec	$\Delta \dot{w}_2 = 21$ lb/sec
$\Delta W_1 = -24{,}472$ lb	$\Delta W_2 = -4167$ lb
$\Delta w_1 = -20{,}304$ lb	$\Delta w_2 = -3493$ lb

With the new payload, the "scaled" booster trajectory was simulated and, as expected, was identical with the nominal trajectory. For this example we took $\mu_1 = \mu_2 = 0.26$.

Reference

[1] Koelle, H. H., *Handbook of Astronautical Engineering* (McGraw-Hill Book Co., Inc., New York, 1961), pp. 20-1–20-9.

Unsteady Flow Past Junctures in Ducts

A. G. Hammitt* and H. J. Carpenter†
TRW Space Technology Laboratories, Redondo Beach, Calif.

The problem of shock waves in ducts is one that is important to bomb shelter installations that use some sort of ventilation or other piping system connecting to the atmosphere. Although these systems are relatively simple from a plumbing point of view, they are generally beyond the state of the art of standard one-dimensional flow analysis. In particular, they usually contain L and T junctures for which standard one-dimensional flow analyses are not available.

The purpose of this note is to set up the boundary conditions to be applied at such discontinuities to fit into a one-dimensional unsteady flow analysis. The detailed, non-one-dimensional flow pattern near the juncture will be ignored, but the effect a few diameters away, where the flow has become one-dimensional again, will be described. The viscous and shock losses that occur near the junctures will be summed up by (over-all) loss coefficients. These loss coefficients can be obtained from steady flow data and used to predict the losses for the unsteady cases. Although the treatment of the flow at the junctures is empirical with regard to these loss coefficients, it is the best that can be expected within the framework of one-dimensional inviscid theory. A true de-

Received July 21, 1964.

* Manager, Aerosciences Laboratory Research Staff. Member AIAA.

† Member of Technical Staff. Member AIAA.

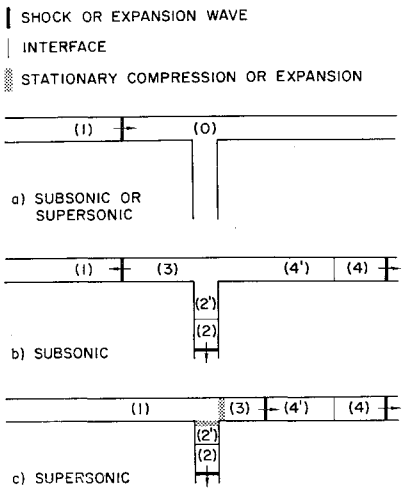

Fig. 1 Wave motion in T juncture.

scription of the flow cannot be obtained without considering both three-dimensional and viscous effects, which is beyond present technology.

To demonstrate the analysis, the case of a T juncture will be considered. Figure 1 shows the situation both before and after the shock wave reaches the T. Two cases must be considered; these are when flow velocities behind the initial shock wave are subsonic (Figs. 1a and 1b) and supersonic (Figs. 1a and 1c). In either case, there are a limited number of disturbances that can exist in the flow. In Fig. 1a, a shock wave is shown moving down the duct toward the T. There is no flow ahead of this shock (0) and subsonic flow behind (1). Figure 1b shows the situation that must exist after the flow has passed through the T juncture. There are transmitted shocks passing down the two legs of the T with conditions (2) and (2′) and (4) and (4′) behind them, the primed and unprimed quantities being those on separate sides of the entropy discontinuity. There can be steady-state phenomena standing in each leg of the T at the T and a reflected wave moving upstream with condition (3) behind it.

Figure 1a is also the initial picture for the supersonic case, and Fig. 1c gives the situation after the shock has passed through the T, the difference being that the upstream propagating wave is now swept down the straight leg of the T since the velocity here is supersonic. For the case illustrated, the perpendicular leg of the T is not supersonic, and so no upstream propagating wave can be swept down it, but the case where it is supersonic could easily be considered.

In the present analysis, the steady phenomena at the juncture will have loss coefficients assigned to them. These loss coefficients will be picked from incompressible steady-state results, the only ones available, and then the predicted results checked against shock-tube experiments.

The method of solution is best illustrated on a pressure-velocity (p-u) diagram. Figures 2a and 2b show these diagrams for both subsonic and supersonic cases. These two diagrams are self-explanatory when studied with reference to Fig. 1. The loss coefficients for the flow that turns into the vertical leg has been taken as one dynamic head based on the flow velocity ahead of the T and one-half the dynamic head

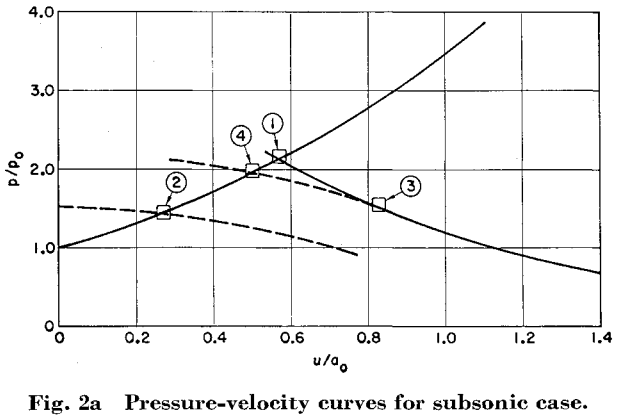

Fig. 2a Pressure-velocity curves for subsonic case.

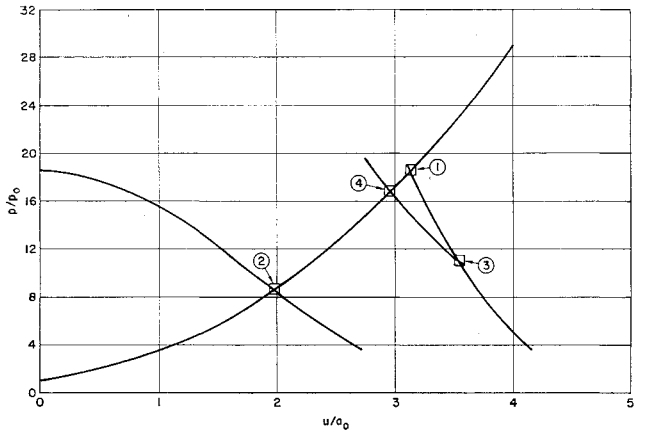

Fig. 2b Pressure-velocity curves for supersonic case.

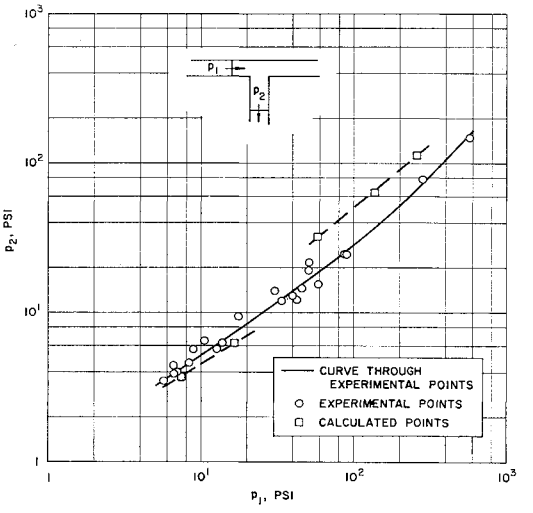

Fig. 3a Incident vs transmitted overpressure in the perpendicular leg of T.

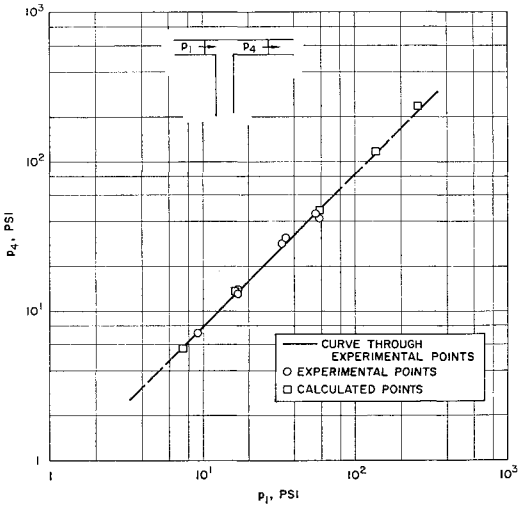

Fig. 3b Incident vs transmitted overpressure past T.

based on the flow velocity in the vertical leg. This loss is shown on Fig. 2 by starting the p-u curve for the flow entering the vertical leg from zero velocity instead of from the actual velocity that exists and constructing the curve to show a loss of one-half the dynamic head. The losses specified in this way are consistent with the two limiting cases of no flow into the vertical leg, where static pressure should exist, and flow from zero velocity in the straight tube, where the loss based on the inflow dynamic head is taken because of the poor inlet configuration.

The solutions can now be carried out by assuming different shock strengths and then using the continuity relation at the T juncture to determine the relative area ratios appropriate to the conditions assumed. If a particular area ratio is desired, different conditions can be assumed until the required area ratio is obtained. The conditions shown correspond to equal areas in all legs of the T.

Calculations for a T configuration with equal area legs have been made for various shock strengths and the losses as assumed previously (Fig. 3). Compared with experimental measurements made in the reference, the agreement is reasonable for both subsonic and supersonic cases. Other values of the loss coefficients, particularly higher values of the loss coefficient based on the inflow dynamic head for the supersonic cases, would give better results. Measurement of these losses by steady-state experiments would be useful. For initial shock strengths that give Mach numbers near 1 ($P_s \sim$ 56 psi), no solution is possible using the loss coefficients selected, indicating that they are not correct for these Mach numbers. The extension of this model to L junctures and other configurations is obvious and will not be considered here.

One use of this model is to correlate the experimental data, such as in Ref. 1, in terms of a few loss coefficients and to provide a tool for extrapolating to other values of initial shock strength. Its more important use is to provide a boundary condition at the juncture to use in unsteady flow calculations by the method of characteristics. Empirical data will probably never be available to provide the detailed information of what happens as waves of different types (such as multiple reflections due to the downstream configuration of the two legs) impinge upon the T and some analytic model such as this one is required to provide a self consistent boundary condition.

Reference

[1] "Information summary of blast patterns in tunnels and chambers," Ballistic Research Labs. Memo. Rept. 1390, 2nd ed. Defense Atomic Support Agency Rept. 1273 (March 1962).

Model Law for Parachute Opening Shock

KENNETH E. FRENCH*
Lockheed Missiles and Space Company, Sunnyvale, Calif.

Nomenclature

C_D = drag coefficient, dimensionless
D_0 = canopy constructed diameter, ft
F = net force on system, lb
F_p = peak opening shock, lb
f_j = functional relationship (j = 1, 2)
g = acceleration of gravity, ft/sec^2
k = coefficient of proportionality, dimensionless
l_s = parachute suspension-line length, ft
M = mass of chute plus mass of attached load, slug

Received July 20, 1964.
* Research Specialist. Member AIAA.

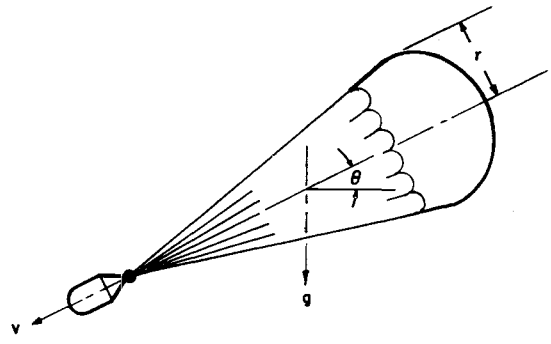

Fig. 1 Diagram of system.

m_{air} = mass of air within and associated with inflating chute, slug
q = instantaneous dynamic pressure, lb/ft^2
q_0 = dynamic pressure at beginning of inflation, lb/ft^2
R = maximum projected radius of fully inflated chute, ft
r = instantaneous value for chute maximum projected radius, ft
r_0 = chute maximum projected radius at beginning of inflation, ft
S = πr^2 = chute reference drag area, ft^2
S_0 = $\pi D_0^2/4$ = chute reference drag area based on canopy cloth area, ft^2
v = instantaneous value of velocity, fps
v_0 = velocity at beginning of inflation, fps
θ = angle of inclination to the horizontal, deg or rad
π = a pure number = 3.14...
ρ = atmospheric mass density, slug/ft^3

Introduction

PARACHUTE opening shock, the maximum force developed during inflation of a parachute, has been the subject of several theoretical investigations (for additional references on opening shock see Ref. 1, pp. 272–274). Of these, Pounder's excellent work[2] appears to provide the most rational and thorough analysis. In view of the date of Pounder's work (1956), it is somewhat surprising that no model law for parachute opening shock is currently regarded as acceptable.[3] The lack of application of Pounder's work is apparently due to its mathematical complexity and its requirement for rather good test data on the inflation sequence for a particular type of parachute. Because of these obstacles to rapid, practical application of Pounder's theory, it is desirable to develop simple, approximate scaling laws for parachute opening shock. Such a development and its correlation with test data are the subjects of this paper.

Dimensional Analysis

Consider the problem of dynamical similarity in determining peak opening shock in the testing of a parachute. For simplicity, assume that the parachute inflates along a flight path of constant inclination and that the suspended load has

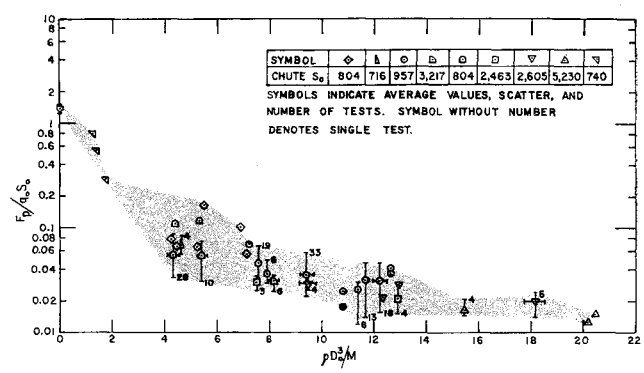

Fig. 2 Euler number vs mass ratio.